Post-Eocene Rhinocerotid Dispersal via the North Atlantic

Danielle Fraser[1,2,3,4], Natalia Rybczynski[1,2,3], Marisa Gilbert[1], and Mary R. Dawson[5]

[1]Palaeobiology, Canadian Museum of Nature, PO Box 3443 Stn "D", Ottawa ON K1P 6P4

[2]Department of Biology, Carleton University, 1125 Colonel By Drive, Ottawa, Ontario, Canada K1S 5B6

[3]Department of Earth Sciences, Carleton University, 1125 Colonel By Drive, Ottawa, Ontario, Canada K1S 5B6

[4]Department of Paleobiology, Smithsonian National Museum of Natural History, Washington, DC, 20560, USA

[5]Vertebrate Paleontology, Carnegie Museum of Natural History, 4400 Forbes Ave, Pittsburgh, PA 15213, United States

Abstract

The North Atlantic Land Bridge (NALB), which connected Europe to North America, enabled high latitude dispersal, particularly during globally warm periods such as the Paleocene-Eocene Thermal Maximum, a period of dramatic faunal reorganization. It has been generally accepted that the NALB was submerged by the early Eocene. Herein, we describe a new rhinocerotid species from the early Miocene of the Canadian High Arctic with proximity to the NALB and present a novel phylogenetic hypothesis for rhinocerotids. We model a high number of dispersals between Europe and North America, some of which occurred in the Oligo-Miocene, suggesting that the NALB may have been crossable for mammals millions of years longer than previously considered. Moreover, recent geological and palaeoclimatological evidence suggest that, until the Miocene, portions of the NALB may have been separated only by narrow and shallow waterways and, potentially, bridged by seasonal sea ice as early as the late Eocene, enabling rhinocerotid dispersal. We thus provide insight into the importance of the Arctic as a persistent connector of otherwise geographically disparate faunas that played a pivotal role in mammalian evolution.

Introduction

Biotic interchange (i.e., the movement of organisms among regions and continents) has occurred innumerable times throughout the history of life, enabled by various mechanisms, including episodic geographical rearrangements and climate changes that reduced barriers to dispersal (e.g., the Bering Land Bridge during the Cenozoic)[1,2]. Biotic interchange enables clades to colonize new environments and diversify to fill new ecological niches (e.g.,[3,4]). It brings species into contact that otherwise would not be and can trigger profound changes to ecosystems through enhanced species richness, extinction of endemics, and alteration of the numbers and types of biotic interactions among organisms (e.g.,[5-12]). Biotic interchange has therefore structured species assemblages over large spatiotemporal scales, ultimately leading to the distributions of organisms as we know them today (e.g.,[6,8]).

Cenozoic terrestrial mammalian faunas have been shaped and re-shaped globally through biotic interchange across the land bridges of the Arctic and subarctic (e.g.,[13-19]). During the Paleocene, the presence of land bridges in combination with warm climates drove the synchronous appearance of new mammal taxa across multiple continents[20-22]. Simpson [23] recognized that mammals dispersed among the Northern Hemisphere landmasses based on patterns of faunal similarity but, at the time, considered only a single dispersal route, the Bering Land Bridge. It is now clear that biotic interchange among the Northern Hemispheric continents occurred over three possible routes, one via the Bering Strait and two via the North Atlantic (i.e., the Thulean and De Geer routes, collectively the North Atlantic Land Bridge or NALB)[24-27].

Time-calibrated molecular phylogenies suggest that there were repeated dispersals via the Bering Land Bridge that peaked during the Oligo-Miocene and coincided with periods of

climate change[28]. Fossil mammal and plant occurrences similarly suggest repeated dispersal events, necessitating that the Bering Land Bridge was crossable through much of the Cenozoic[29-31]. A series of fossil discoveries from the Arctic show that biotic interchange via the Bering Land Bridge played a pivotal role in Late Neogene mammal evolution until regional subsidence led to the opening of the Bering Strait 5.5-5.4 Ma[32-36]. Thereafter, biotic interchange was paced by the episodic formation of the Bering Land Bridge due to Pleistocene fluctuations in land ice volume and, thus, sea level[37,38], shaping the population genetics of extant species such as wolves (*Canis lupus*), lions (*Panthera* sp.), and brown bears (*Ursus arctos*)[39,40].

Much of the evidence for biotic interchange via the North Atlantic comes from mid latitude floral and faunal comparisons between North America and Europe[41,42]. The early Eocene faunas of the Eureka Sound Formation of Ellesmere Island also strongly resemble the contemporary faunas of Western Europe, supporting some degree of North Atlantic faunal continuity[43-45]. Dispersal over the NALB occurred via two routes, the De Geer and Thulean routes[25,26,46,47]. The De Geer route required crossing from Northern Europe over Svalbard and Greenland to Ellesmere Island and formed a continuous land bridge during the Paleocene[24-27,31,45,46,48-50]. The more southerly Thulean route, which connected Britain to North America via the Greenland-Iceland-Faroe Ridge, was traversable during the late Paleocene through early Eocene[24-26,41,46,51-58]. While the NALB likely played an important role in biotic interchange during the early Cenozoic, post-Eocene dispersal via the North Atlantic has not typically been considered to have occurred with significant frequency. Furthermore, for most terrestrial groups, we lack a thorough understanding of their biogeographic history regarding when and how frequently dispersal may have occurred and via which routes.

The historical geographic range of extant rhinocerotids encompassed Southern Asia and Africa[59-62]. Rhinocerotids, however, achieved a near global distribution during the Cenozoic, coming to occupy North America, Europe, Asia, and Africa[63,64], implying a complex biogeographic history. The earliest rhinocerotoids (i.e., *Uintaceras*) colonized North America from Eurasia during the middle Eocene (~47 Ma)[63]. Thereafter, one or more dispersals occurred from North America to Eurasia, setting up the conditions for the evolution of the rich Cenozoic rhinocerotid faunas of the Eastern Hemisphere. Dispersals within Asia and between Europe and Asia were common thereafter, during the last 30 Ma[64].

Herein, we briefly describe a near complete specimen (~75%) belonging to new rhinocerotid species from the Haughton Astrobleme, an impact crater located in the Canadian Arctic Archipelago with proximity to the NALB. The Haughton Astrobleme is an extraterrestrial impact crater located near the north-central coast of Devon Island, Nunavut, Canada[65]. The age of the impact is uncertain. The impact event was originally ascribed a ~23 Ma cooling age based on $^{40}Ar/^{39}Ar$ dating [66] and apatite fission track thermochronology [67]. However, it was revised to 39 Ma using a spot-dating $^{40}Ar/^{39}Ar$ approach on glass within the gneiss[68], 23 Ma based on (U-Th)/He ages from zircons[69], and 31 Ma based on $^{40}Ar/^{39}Ar$ ages from shocked feldspar clasts[70]. Within the crater is the Haughton Formation, a lake deposit preserving pollen, megaflora, and vertebrate fossil remains[71] (see *Supplementary Text*). Occurrences of ?*Desmatolagus schizopetrus*[72] and a shrew belonging to the subfamily Heterosoricinae with resemblance to *Wilsonosorex*[73] support a Hemingfordian (20.43 – 15.97 Ma) age for the Haughton Crater fauna. The pinniped discovered in the crater, *Puijila darwini*[74], is also a close relative of the well-known European genus, *Potamotherium*, which occurs between ~24 – 19 Ma[75]. Furthermore, the presence of Graminae pollen in combination

with *Acer* (maple) and *Tilia* (lindens and basswoods) suggests an age between Miocene and Pliocene[76,77]. Thus, we consider the impact age of ~23 Ma a maximum age for the lake deposits that is most consistent with the faunal assemblage.

Relatively little is understood about rhinocerotid biogeography on a global scale, particularly relating to dispersal among the Northern Hemisphere continents, owing largely to the lack of a global-scale phylogenetic hypothesis. To this end, we present a novel phylogenetic hypothesis for rhinocerotids. To simultaneously infer tree topology and divergence times, we perform a combined evidence analysis for stratigraphic range data using a fossilized birth-death model, a sampling model that describes how speciation, extinction, and sampling produce a given phylogeny[78,79], implemented in RevBayes[80]. We compiled morphological character matrices and scored morphological characters for additional North American species. We also downloaded cytochrome B sequences for all extant rhinocerotids (see *Methods*). Our final dataset included 57 species of rhinocerotid, representing most of the presently named genera. We generated the tree topology based on estimated dates of the Haughton impact of ~23 Ma[66,67,69].

Finally, to characterize the timing and number of dispersals, we perform a global-scale analysis of rhinocerotid historical biogeography using the maximum likelihood approach available in the BioGeoBears R package[81-83]. To test for differences in dispersal rates among regions, we used Biogeographical Stochastic Mapping[81-84] (see *Methods*). The present study provides, to the best of our knowledge, the most taxonomically inclusive and spatially extensive study of rhinocerotid biogeographic history.

We find that the Haughton rhinocerotid represents a North Atlantic dispersal event no earlier than the latest Eocene and that rhinocerotids underwent repeated dispersals via the

North Atlantic, including during the Oligo-Miocene. Ours is the first evidence of a persistent NALB supported by the fossil record of the evolution of a terrestrial vertebrate. What is emerging is a picture of a NALB that played a much larger role in mammal dispersal than previously recognized, prompting a reevaluation of our understanding of Northern Hemisphere mammalian evolution.

Systematic palaeontology

Perissodactyla Owen, 1848

Rhinocerotoidea Owen, 1845

Rhinocerotidae Gray, 1821

Epiaceratherium Abel, 1910

Epiaceratherium itjilik Fraser et al., spec. nov.

Genotypic Species

Epiaceratherium bolcense Abel, 1910

Included Species

Epiaceratherium bolcense Abel, 1910, *Epiaceratherium itjilik* Fraser et al., sp. nov., *Epiaceratherium magnum* Uhlig, 1999, *Epiaceratherium naduongense* Böhme et al., 2013.

Geographical Distribution

Northern Vietnam, Pakistan, Czech Republic, Northern Italy, Germany, Switzerland, France, and the High Arctic of Canada.

Stratigraphic Distribution

Late Middle Eocene to Early Oligocene (South Asia), Early to early Late Oligocene (Europe), and late Oligocene or early Miocene (Canada).

Etomology

itjilik (Inuktitut): frost or frosty, in reference to the fact that the specimen was collected in the High Arctic of Canada, which is, today, characterized by cold climates that support glaciers and permafrost.

Holotype

CMNFV 59632

Diagnosis

Epiaceratherium is a stem rhinocerotine lacking i3 and a lower canine, with a wide postfossette on P2–P4, a protoloph usually constricted on M1–M2, a straight posterior half of the ectoloph on M1–M2, and a posterior valley usually closed on p2.

Emended diagnosis

Epiaceratherium itjilik possesses a fused protocone and hypocone of the P2, an interrupted P3 protoloph, the presence of a medifossette on the upper molars, absence of a lingual cingulum on the upper molars, and a low and interrupted posterior cingulum on the M1-2.

Description

The nearly complete skeleton of one individual was found over a surface area measuring 5 – 7 m. The bones occurred both as surface lag and within the active layer, above the permafrost. The specimen preserves left and right mandibulae and maxillae. The cheek teeth are erupted and in wear (Fig. 1; *Supplementary Figures* 1-2), suggesting early to mid adulthood, which is corroborated by the closure of the long bone epiphyses. Remains of the skull are restricted to the posterio-dorsal portions of the brain case and right zygomatic arch, partial skull roof, incomplete foramen magnum, braincase floor, and portion of the left zygomatic arch. Portions of the nasal bones are also preserved, lacking rugosity, suggesting the absence of a horn (*Supplementary Figure* 1).

Epiaceratherium itjilik sp. nov. possesses a low zygomatic arch, smooth jugal/squamosal suture, a depression between the temporal and nuchal crests, fused nasal bones, a lingual groove on the corpus mandibulae, and a mandibular ramus that is inclined forward. The mandibular symphysis is transversely narrow, extending posteriorly in line with the alveolus for the talonid of the p1. A mental foramen occurs on the lateral sides of the mandibulae, aligned with the p3. The left mandible bears crowns of p3, p4, and m2 and the right mandible crowns of p3-m3, though the m1-m3 crowns are broken to varying degrees (*Supplementary Figure* 2). Alveoli for i1 and i2 are preserved. The i2 is a tusk with a nearly horizontal root (*Supplementary Figure* 2). There are no alveoli or roots for an i3 or lower canine. The right p1 is preserved as an isolated tooth and posseses two roots. Only the alveolus remains of p2, which posseses a narrower trigonid than talonid. The other lower teeth are characterized by long paralophids and the presence of labial cingula on the lower molars.

The maxillae are well preserved; the left maxilla preserves the P2-M3, though the M1 is heavily damaged. The right maxilla similarly preserves the P2-M3, though the labial aspects of the P4 and M1 are damaged (Fig. 1; *Supplementary Figure* 3). Though the P1 is not preserved, the anterior root is small and rounded while the posterior root is transversely wide. The P2 is submolariform. The P3 is smaller than the P4. The M2 and M3 bear distinct parastyles. The dentition lacks cement and the upper premolars lack a labial cingulum, though the P2-4 sometimes possess a lingual cingulum. The protocone and hypocone of the P2-4 are fused. There is an antecrochet on the P3, a low and interrupted posterior lingual cingulum on the M1-2, and presence of a labial cingulum on the lower molars.

A large portion of the post-cranial sckeleton is also preserved, including a partial atlas and axis, humeri, radii, ulnae, scapulae, femora, ribs, left forefoot, left and right hindfeet, several

thoracic and lumbar vertebrate, and an incomplete pelvis. The manus and pes possess the nearly complete complement of carpals and tarsals (*Supplementary Figures* 4-5). All postcranial bones except some of the manus and pes are broken, possibly due to freeze and thaw action of the permafrost, before collection. The carpals of *E. itjilik* are large and deep. The manus bares a fifth metacarpal (*Supplementary Figure* 4). The femur has no third trochanter. There is a small rough facet in its place. The atlas facets on the axis are straight, the scapula is very elongated, the radius and ulna are in contact, presence of an anterior tubercle on the distal end of the ulna, the anterior height of the scaphoid is less than the posterior height, the anterior side of the semilunate is keeled, the proximal facet of the McIV is trapezoid in shape, the medio-distal gutter of the tibia is shallow, the posterior apophysis of the tibia is low, the proximal articulation of the femur is high, the depth to height ratio of the astragalus is less than 1.2, the fibula facet of the astragalus is subvertical, presence of an expansion of the first calcaneus facet on the astragalus, and insertion of the m. interossei on the lateral metapodials is short.

Results

Phylogenetic analysis. — Our phylogenetic analyses recover *Epiaceratherium itjilik* as a member of the genus *Epiaceratherium* and sister taxon to *E. magnus* and *E. delemontense*, two species found in Europe plus the Middle East and Europe, respectively, with a divergence date of ~40.5 Ma to ~34.4 Ma (Fig. 2; *Supplementary Figure* 6). The fact that *E. itjilik* is sister to two species found in Europe implies dispersal between Europe and North America during the latest Eocene (Fig. 2; *Supplementary Figures* 7-8).

Our phylogenetic analysis included most of the named rhinocerotid genera. The resulting phylogenetic hypotheses are similar, in many ways, to other published hypotheses (e.g.,[64,91-93]). Importantly, we recover Elasmotheriinae and Elasmotheriini[94]. We also reconstruct the split between the Rhinocerotinae and Elasmotheriinae between ~38.7 Ma and ~34.1 Ma

(*Supplementary Figure* 6), which is more recent than recently proposed[95]. Unexpectedly, we reconstruct *Parelasmotherium schansiense* as a sampled ancestor to *Elasmotherium sibiricum* and *Sinotherium lagrelii* with a moderate posterior probability (0.52; *Supplementary Figure* 6).

Biogeographic analyses. — The best fit biogeographic model was either the DEC model or the DIVALIKE model with jump dispersal (Table 1; *Supplementary Tables* 1-2). Employing biogeographic stochastic mapping under each model suggests the occurrence of numerous dispersal events among all biogeographic regions except Africa (Fig. 2-3; *Supplementary Figures* 7-8). Under both unstratified and stratified models, the greatest number of dispersals occurred between Europe and the Middle East (Fig. 3). Under an unstratified model, the number of dispersals directly between Europe and North America (i.e., total in both directions) nears the same magnitude as between Europe and Asia (Fig. 3A). Under a stratified model where the North Atlantic Land Bridge (NALB) was crossable until 21 Ma, the number of dispersals between Europe and North America is marginally greater than for Europe and Asia (Fig. 3B). Notably, dispersals between Europe and North America are reconstructed as occurring as late as the early Miocene (Fig. 2; *Supplementary Figures* 7-8). However, under a model where the NALB was only crossable until 35 Ma, the number of dispersals between Europe and North America is approximately half of that for Europe and Asia (Fig. 3C). Under all model types, dispersals between Asia and North America are low (Fig. 3), despite the Bering Land Bridge being accessible intermittently until 5.5-5.4 Ma[32].

Discussion

Dispersal of terrestrial organisms via the North Atlantic during the Paleocene and early Eocene is well-established based on floral and faunal similarity between mid-latitude Europe and North America[20-23,41,42]. Subsequent cessation of North Atlantic land-based dispersal during the early

Eocene has been inferred from enhanced faunal dissimilarity as well as geological models that suggested simultaneous opening of waterways between the Arctic Ocean and North Atlantic (reviewed by Brikiatis [24]). Owing to the lack of global-scale phylogenetic hypotheses for most terrestrial taxa, however, knowledge of biogeographic histories (i.e., when, how often, and via which routes taxa may have dispersed) has also been woefully limited. Herein, we describe a new rhinocerotid, *Epiaceratherium itjilik* Fraser et al. sp. nov., from the Haughton Formation of Devon Island. We also present global-scale biogeographic analyses based on a novel time scaled phylogenetic hypothesis for rhinocerotids. We find that the Haughton rhinocerotid represents a North Atlantic dispersal event no earlier than the latest Eocene and that rhinocerotids underwent repeated dispersals via the North Atlantic, including during the Oligo-Miocene, necessitating a reevaluation of terrestrial dispersal via the North Atlantic during the Cenozoic.

Epiaceratherium is a genus of rhinocerotids with four previously described species from the Oligocene [88-90,92]. The Haughton Crater rhinocerotid is diagnosable as *Epiaceratherium* but differentiated from existing species by characteristics of the P2, P3, and upper molars (see *Emended Diagnosis*), necessitating the erection of a new species, *Epiaceratherium itjilik* Fraser et al. sp. nov. The occurrence of *E. itjilik* in the Haughton Crater significantly extends the duration of *Epiaceratherium* by millions of years, given an estimated maximum age of 23 Ma[66,67,69]. Its geographic range is also expanded to North America, making it one of the most widespread rhinocerotid genera. *E. itjilik* also represents the highest latitude record of a rhinocerotid, to date, and the first occurrence in the Canadian Arctic Archipelago. The presence of rhinocerotids in the Western Low Arctic (i.e., Yukon Territory) during the Tertiary is apparent based on an enamel fragment that is not identifiable to genus or species[96]; the much higher latitude occurrence of *E. itjilik* reported herein is represented by a nearly complete skeleton. The

presence of a rhinocerotid in the High Arctic represents an interesting palaeoecological puzzle. Though the flora of the Haughton Crater suggests a temperate palaeoclimate[71,76], there would have been a near modern light regime with months long periods of darkness. Analysis of palaeodiet and migration patterns using tooth wear and stable isotopes may, in the future, illuminate the ecological strategies of high latitude herbivores during the period of deposition of the Haughton Formation.

Phylogenetic analysis based on a fossilized birth-death model reconstructs *E. itjilik* as sister to *E. delemontense* plus *E. magnum*, two species with geographic ranges including Europe, with an estimated divergence date of ~40 Ma to ~34 Ma (Fig. 2; *Supplementary Figure* 6). *E. itjilik* therefore likely represents the outcome of a dispersal event between Europe and North America during the latest Eocene. Our global-scale biogeographic analyses show that rhinocerotids, in fact, underwent repeated intercontinental dispersals (Fig. 2-3), illuminating a much more complex history than previously known. There were repeated dispersals among Europe, Asia, and the Middle East during the Oligo-Miocene. Direct dispersal between North America and Europe occurred with surprisingly high frequency, second only to dispersals within Eurasia (i.e., Europe, Asia, and the Middle East) (Fig. 3). The oldest Europe to North America dispersal occurred no earlier than the divergence of *Epiaceratherium itjilik* from *E. delemontense* plus *E. magnum* (Fig. 2), during the latest Eocene. The most recent occurred during the Miocene, involving the ancestors of taxa including *Teleoceras* as well as *Peraceras*, and *Aphelops* (Fig. 2), common North American Miocene rhinocerotids [63]. Employing various possible dates (i.e., 35 Ma and 21 Ma) for the opening of impassable North Atlantic waterways and models of dispersal does not change the overall pattern (Fig. 3; *Supplementary Figures* 7-8). Rhinocerotids represent the first set of modelled post-Eocene land dispersals among vertebrates via the NALB. Our

phylogenetic analysis and biogeographic analyses thus reconstruct dispersals that have otherwise been considered unlikely by palaeontologists (e.g.,[23,27,41,42,52]).

Rhinocerotids are, however, not the first known cases of post-Eocene dispersal via the North Atlantic. A number of plant fossils indicate that the NALB persisted beyond the Eocene; occurrences of nuts and leaves of two species of *Fagus* (i.e., beech) on Iceland suggest that one dispersed from North America and the other from Europe during the late Miocene[97]. Pollen of Oaks (i.e., *Quercus*) from the late Miocene sediments of Iceland also suggest biotic interchange much later than the Eocene[98]. Similarly, the common ancestors of *Perca* and *Sander*, two genera of freshwater perch, were continuously distributed across the North Atlantic Land Bridge (NALB) until the mid-Miocene, after which their respective species diverged[99-101]. Whereas oak pollen may have been distributed to Iceland via wind, the seeds of *Fagus* are not distributed long distances (~95% disperse within 25 m of the parent plant)[102], necessitating some degree of land continuity until the Miocene. A continuous distribution of freshwater fish across the NALB also suggests the presence of contiguous freshwater connections until the Miocene, consistent with our biogeographic models for rhinocerotids.

Terrestrial crossing via the NALB occurred via the De Geer and Thulean routes[24-26,46,47]. Dispersal via the De Geer route required organisms to cross from Sweden and Norway (i.e., Fennoscandia) to Svalbard, Greenland, and then Ellesmere Island[25,26]. Terrestrial crossing via the De Geer route (~75°N) is currently impeded, from east to west, by the Barents Sea, Fram Strait, and Nares Strait[26]. The Fram Strait and Barents Sea currently present the greatest barriers. Dispersal via the more southerly Thulean route (~65°N) involved crossing the North Atlantic via the Greenland-Iceland-Faroe Ridge Complex, which formed a land connection between Scotland and Greenland over Iceland[25,26]. Terrestrial crossing via the Thulean route is currently impeded

by the Iceland-Faroe Ridge, Feroe-Shetland Channel, Denmark Strait, and Nares Strait[26]. There are numerous and variable dates for the submergence of the NALB, based on faunal, floral, palaeoclimate, and geological evidence[24,103].

Brikiatis [24] considered the De Geer route definitively subaerial from the latest Cretaceous to early Palaeocene based on geotectonics and palaeogeography that suggest the Barents Shelf was submerged by the mid Paleocene. The formation of the De Geer route explains faunal similarities between Eurasia and North America during the early Paleocene (e.g.,[13-19]). Paleobathymetric reconstructions, however, suggest a land connection between Fennoscandia and Svalbard traversed the Barents Seaway until the Quaternary[104]. The Fram Strait was thus the only gateway connecting the Arctic and Atlantic Oceans post-Eocene. Today, the Fram strait provides the only deep-water connection between the Atlantic and Arctic oceans and is pivotal in the formation of North Atlantic Deep-Water, Atlantic Meridional Overturning Circulation, and, thus, climate evolution during the late Cenozoic[105]. Dates for the formation of deep water in the Fram Strait based on seismic data, tectonic models, sedimentation rate estimates, and aeromagnetic surveys range from ~21 Ma to ~14 Ma (i.e., the Miocene)[103]. Despite the large discrepancy in estimates for the timing of deep-water formation, the Fram Strait was likely shallow and narrow until at least the earliest Miocene[103,105-111]. The De Geer Route was therefore potentially intact or interrupted only by shallow waterways prior to the Miocene, presenting relatively little impedance to terrestrial dispersal relative to today.

Brikiatis [24] considered the De Geer and Thulean routes as non-contemporaneous, reconstructing the Thulean route as subaerial during the latest Paleocene and earliest Eocene based on seismic, stratigraphic, and vertebrate occurrence data. The formation of the Thulean route explains the enhanced similarity of mammalian faunas during the Paleocene-Eocene

328 Thermal Maximum (e.g.,[22]). Estimates for the timing of the submergence of the Thulean route
329 are, however, highly variable ranging from 35 Ma to 6 Ma based on vertebrate occurrences,
330 geophysical modelling, benthic foraminifera, and plant fossils, among others[25,26,54,98,112-114].
331 Vertebrate and geological evidence suggest that the Faroe-Shetland channel likely opened first,
332 during the late Eocene or early Oligocene[25,26,112,113] but, possibly, as late as the Miocene[114,115]
333 and that the Iceland-Feroe and Greenland-Iceland Ridges were subsequently submerged between
334 the late Oligocene and early to late Miocene[112-118]. Thus, it is apparent that the Thulean route was
335 likely crossable for much longer than has been previously considered, consistent with our
336 biogeographic models for rhinocerotids.
337 Today, Devon Island is located within the Canadian Arctic Archipelago, which was
338 formed during the Quaternary when glacial activity resulted in the deepening of the drainage
339 pattern of what was originally a contiguous land mass[119]. The final leg of dispersal from Europe
340 to North America would thus have been the Nares Strait, a waterway separating Devon Island
341 from Greenland. Absent during the Cretaceous due to the presence of a contiguous landmass
342 comprised of Greenland and Ellesmere Island, the Nares Strait was formed in two phases,
343 northeasterly movement of Greenland during the Paleocene followed by northwesterly plate
344 convergence, opening, and then narrowing the Nares Strait[120]. Thus, by the Eocene, the Nares
345 Strait would have presented a not insubstantial barrier to dispersal between Europe and North
346 America via the NALB. During the Oligocene and early Miocene, terrestrial organisms
347 dispersing between Europe to North America via the NALB therefore likely would have crossed
348 at least two narrow waterways (i.e., the Fram Strait and Nares Strait or Faroe-Shetland channel
349 and Nares Strait). While it is not entirely impossible that rhinocerotids dispersed via swimming,

we hypothesize that another mechanism explains the commonness of their dispersal between Europe and North America.

During the Paleocene and much of the Eocene, the Northern Hemisphere was very likely ice-free year-round[121-124]; estimates of shallow marine temperatures between 11 and 22 °C are consistent with an ice-free Arctic Ocean[125]. During these ice-free periods, terrestrial mammals would have required contiguous land connections with limited interruption by waterways to disperse between Europe and North America. The subsequent transition from the globally warm hothouse (i.e., Paleocene through late Eocene) to the global cool house (i.e., Oligocene through to Pliocene), driven by decreasing atmospheric CO_2, resulted in the seasonal formation of sea ice in the Arctic Ocean and North Atlantic during the Oligocene and eventual formation of perennial ice, likely during the late Miocene[121-123,126]. Sub-Arctic Ice-Rafted Debris (IRD) records suggest that perennial Northern Hemisphere glaciation commenced during the late middle Miocene (~14 Ma)[123,127]. However, significant amounts of IRD occur in the ACEX sedimentary sequence, pushing the onset of seasonal ice back to the middle Eocene (47 – 46 Ma or 44 – 41 Ma)[128-131], which is supported by estimates of sea surface temperatures (SST) from micropalaeontology[132] and IRD data from ODP Site 913 from the Greenland Basin[133-135]. ACEX SST estimates similarly suggest that sea ice was present in the Arctic Ocean after 45 Ma, reflecting enhanced seasonality[123,124]. We therefore suggest that winter sea ice may have provided seasonal dispersal routes for terrestrial mammals as early as the late Eocene. Thus, the picture that is emerging is one of a NALB that may have been crossable by terrestrial animals into the mid Cenozoic and, possibly, the Neogene.

While ice may have provided a physical means of crossing the NALB after the early Eocene, the drivers of such dispersals are unresolved. Highly seasonal environments with harsh

winters, particularly after the Eocene-Oligocene Transition (EOT; ~34.1 – 33.55 Ma), a period marked by global cooling and enhanced seasonality[121,122,136], should have impeded dispersal even in the presence of land bridges. However, *Epiaceratherium itjilik* represents a dispersal event between Europe and North America that occurred prior to the EOT. Thus, the population(s) that gave rise to *E. itjilik* dispersing during the latest Eocene would not have experienced the much harsher high latitude winters of the EOT and seasonality, therefore, may not have presented an impassable barrier. Furthermore, Oligocene climates appear to be distinct in that they were associated both with the significant growth of polar ice, particularly in the southern hemisphere, and anomalously warm high latitudes[126]. Similarly, mid Miocene high latitudes were comparatively warm, despite the apparent presence of at least seasonal glaciation[123,127,137]. Rhinocerotid dispersal during the Oligo-Miocene may therefore not have been impeded by harsh high latitude climatic conditions. However, harsh high latitude winters may not impede such dispersal as much as expected. For example, living ungulates (e.g., caribou and Muskox) feed by using their hooves and antlers to dig through ice and snow[138]. These strategies support large, non-migratory herds in the High Arctic through long, cold, and dark winters. Some caribou populations, such as on Svalbard, are also known to feed on washed up seaweed[139], though such diets are not long-term strategies. We thus consider crossing island to island, potentially over multiple seasons, via the North Atlantic a viable scenario for rhinocerotids and, potentially, other terrestrial mammal taxa.

Presently, there are, to our knowledge, no records of post-Eocene terrestrial vertebrate fossils from the islands that comprised the NALB. The discovery of vertebrate or molecular remains in sedimentary rocks of Oligo-Miocene age on Iceland or Greenland would support the findings of the present paper. However, such rocks are rare on both islands, primarily preserving

the remains of invertebrates such as marine bivalves, insects, and plants[98,115,140,141]. Despite the current lack of a vertebrate fossil record confirming our findings, we believe they are not artefactual (e.g., that the Europe to North America dispersals we model represent Europe to Asia to North America dispersals obscured by an incomplete fossil record). Firstly, the rhinocerotid records of eastern Asia are rich (e.g.,[64,91]). Secondly, vertebrate-bearing sedimentary rocks of Oligo-Miocene age are well represented across Asia[142]. Finally, rhinocerotids are large-bodied mammals with a comparatively high probability of entering the fossil record[143,144]. That is, there have been numerous opportunities to discover genera and species filling the gaps between taxa that represent dispersals directly between Europe and North America in our models. While there are certainly new rhinocerotid taxa to discover, we suggest that the number of modelled dispersals directly between Europe and North America are too numerous to all be the result of fossil record incompleteness. The proposal of dramatically different phylogenetic hypotheses could unseat our findings, however, and we welcome reanalysis using the various available algorithms and variations on the Fossilized Birth-Death model.

Herein, we briefly describe the highest latitude occurrence of a rhinocerotid that represents a new species, *Epiaceratherium itjilik*, Fraser et al. spec. nov. We reconstruct *E. itjilik* as sister to two *Epiaceratherium* species with geographic ranges encompassing Europe, implying a direct dispersal into North America as early as the latest Eocene, potentially enabled by high latitude warmth and comparatively low seasonality prior to the Eocene-Oligocene Transition. Modelling of rhinocerotid biogeographic histories employing a new, novel phylogenetic hypothesis shows that they likely dispersed repeatedly between Europe and North America during mid Cenozoic and, potentially, Neogene. Some models of North Atlantic Land Bridge (NALB) tectonic evolution suggest the region was not crossable for terrestrial animals

beyond the Early Eocene. We suggest, based on a series of geological studies, that persistence of the NALB into the late Oligocene or early Miocene, the presence of periodic climate warm periods in combination with the formation of seasonal sea ice facilitated stepwise rhinocerotid dispersal across the NALB. Rhinocerotids thus represent the first vertebrate for which repeated dispersal via the NALB beyond the Eocene is recorded.

Methods

Specimens. — The newly described specimen CMNFV 59632 from the Haughton Impact Crater on Devon Island is housed at the Canadian Museum of Nature, Ottawa, Canada. Other specimens scored for phylogenetic analysis are housed at the American Museum of Natural History and the Museum of Comparative Zoology (*Supplementary Table* 3).

Terminology. — The morpho-anatomical characters described here follow the terminology of Antoine, et al. [94]. The dental abbreviations are as follows: c/C, lower/upper canine; d/D, lower/upper decidual tooth; i/I, lower/ upper incisor; m/M, lower/upper molar; p/P, lower/upper premolar. Measurements are provided in mm.

Phylogenetic analysis. — To simultaneously infer tree topologies and divergence times, we performed combined-evidence analyses for stratigraphic range data using a fossilized birth-death (FBD) model implemented in RevBayes[145,146]. FBD is a sampling model that describes how speciation, extinction, and sampling produce a given phylogeny[78]. FBD models diverge from other methods for inferring tree topologies in that they incorporate fossil ages, either as a series of point observations or temporal ranges, thus ascribing higher likelihoods to tree topologies congruent with the fossil record[79]. FBD models thus eliminate the need for *ad hoc* calibration of node ages and produce estimates that are robust to biased sampling of fossils and extant species.

441 FBD models are comprised of two processes, the birth-death and fossilization
442 processes[79,147]. The parameters of the birth-death process include rates of speciation (λ) and
443 extinction (μ), the origin time (ø) (i.e., the starting time of the stem lineage), and the sampling
444 probability (ρ) (i.e., the probability that an extant species is sampled)[147]. The fossilization
445 process provides a distribution for the sampling of fossil lineages modeled on a Poisson process
446 with rate parameter ψ[147,148]. We used the birth-death range process described by [149].
447 Unknown parameters, λ, μ, and ψ, are sampled via MCMC. In setting up the FBD
448 process, we placed exponential priors on the speciation (λ) and extinction (μ) rates. Each
449 parameter is drawn independently from an exponential distribution with rates equal to 10. The
450 FBD process is conditioned on the origin time ø, specified as a uniform distribution on the origin
451 age. All extant rhinocerotids are sampled, thus ρ = 1.0. FBD models also estimate the probability
452 of ancestor-descendent pairs, which is correlated with turnover rate μ / λ and fossil recovery rate
453 ψ and probably of sampling ρ[147,150].
454 Discrete morphological character changes are represented by the substitution model,
455 branch rate model, and site rate model. The substitution model describes how discrete characters
456 change over time, modeled using a single-rate Mk model[151], which uses a generalized Jukes-
457 Cantor matrix[152] and assumes that state changes occur symmetrically (i.e., character state
458 changes in any direction are equally likely). This a conservative means of modelling discrete
459 morphological character evolution. We used a model where k = 4, given that the characters used
460 in this study have between two and four states. The branch rate model describes variations in the
461 rate of morphological evolution along different branches in the phylogeny. We assumed a strict
462 clock model (i.e., a constant rate of morphological character changed throughout the tree). The

site-rate model describes variation in the rates of evolution among morphological characters. We allowed gamma-distributed rate heterogeneity among characters.

Nucleotide substitution was modeled using a general time-reversible model of nucleotide evolution with rate heterogeneity across sites modeled on a gamma distribution (i.e., the site rate model)[147]. For the branch rate model, we relaxed the assumption of a strict molecular clock[153]. Thus, for the branch rates model, we used an uncorrelated exponential relaxed clock where substitution rates for each lineage were independent and distributed identically according to an exponential distribution.

For the morphological data partition, we compiled morphological character matrices from[64,91,92,94] using the set of characters retained by Becker, et al. [92], which included 214 characters modified from Antoine, et al. [91]. All characters were aligned where character numbers had changed and character state numbers were edited where necessary (e.g., if a character state was scored 0 in one matrix but 1 in another, they were changed to align with the Becker, et al. [92] matrix). We also scored morphological character states for specimens of *Aphelops megalodus*, *Diceratherium armatum*, *Peraceras profectum*, and *Floridaceras whitei* (*Supplementary Table* 3) to include a wider range of North American genera. Character states were also scored for the Haughton Crater rhinocerotid. Our final dataset included 57 species, representing most of the presently named genera. Stratigraphic range data (i.e., first and last appearance dates) were downloaded from the Paleobiology Database or taken from the relevant literature. For the molecular data partition, we downloaded cytochrome B sequences for all extant rhinocerotids from GenBank (*Supplementary Table* 4) and aligned them using ClustalW2 in Jalview[154,155].

Biogeographic analyses. — Each species was scored as living in one or more of five biogeographic regions: North America, Europe, Middle East, Asia, and Africa. Geographic

ranges were taken from searches for individual species in the Paleobiology Database or the published literature. To test for differences in dispersal rates among regions, we used a modelling approach and Biogeographical Stochastic Mapping (BSM) as implemented in the BioGeoBears R package[81-84]. BioGeoBears enables fitting of an array of biogeographic models in a likelihood framework including Dispersal-Extinction Cladogenesis (DEC), Dispersal Vicariance Analysis (DIVA), and Bayesian Inference of Historical Biogeography for Discrete Areas (BayArea). Each of the included models allows for a range of processes as summarized in Matzke [81], which are assigned probabilities and used to calculate the likelihood of the observed geographic range tip data. All three models have two free parameters, the rate of dispersal (*d*) and range contraction or extinction (*e*) as in Matzke [81]. All allow for species to occupy one or more region. All three models allow for anagenesis via range expansion and contraction. The DEC model assumes that daughter species inherit the ancestral range, live in a subset of the ancestral range, or undergo vicariance within one area (but not splitting off multiple areas)[84,156,157]. In contrast, the DIVA model allows for multi-region vicariance but not inheritance of a subset of the ancestral range by a daughter species (subset speciation in Matzke [81])[157]. The BayArea model assumes no range evolution at cladogenesis but allows for sympatry across multiple regions[158]. DEC, DIVA, and BayArea can all also be implemented incorporating founder event speciation, the process whereby a daughter species "jumps" to a new region, a process that may play a significant role in speciation in island systems[82].

Herein, we assumed three possible biogeographic scenarios, the first where the North Atlantic Land Bridge (NALB) was passable for the entire Cenozoic (i.e., an unstratified analysis), until 35 Ma, and until 21 Ma based. We assumed equal probability of biotic interchange among the other biogeographic regions throughout rhinocerotid evolutionary history.

For each scenario, we then fit all three models with and without the founder event or *j* parameter and compared model fit using the Akaike Information Criterion with a correction for small sample sizes (AICc).

We then used the best fit model for Biogeographical Stochastic Mapping (BSM)[83,159]. BSM uses simulation based on likelihood models of geographic range evolution. It performs Ancestral Character Estimation at nodes and simulates potential histories consistent with the observed geographic range tip data. Summarizing the various simulated range evolution histories, BSM can be used to calculate the numbers of different types of biogeographic events[82,84]. We performed 50 simulations and analyzed the total number of dispersal events among all five geographic regions.

Data Availability

Phylogenetic character data for *Aphelops megalodus*, *Diceratherium armatum*, *Peraceras profectum*, and *Floridaceras whitei* were collected by the authors from the American Museum of Natural History and Museum of Comparative Zoology. Specimen numbers are listed in *Supplementary Table* 3. Biogeographic data were collected from the Paleobiology Database (https://paleobiodb.org) or relevant literature. The data used in this study have been deposited in the Github repository (https://github.com/danielleleefraser/rhinocerotids). We will make the data publicly available and create a permanent DOI once the manuscript is accepted. For review purposes, we have included the files with the submission.

Code Availability

The code used for the current study will be available in the Github repository (https://github.com/danielleleefraser/rhinocerotids). We will make the code publicly available

and create a permanent DOI once the manuscript is accepted. For review purposes, we have included the files with the submission.

LITERATURE CITED

1 Vermeij, G. J. When biotas meet: understanding biotic interchange. *Science* **253**, 1099-1104 (1991).

2 Vermeij, G. J. in *Species invasions: insight into ecology, evolution and biogeography* (eds D.F. Sax, J.J. Stachowicz, & S.D. Gaines) 315-339 (Sinauer Associates, 2005).

3 Cantalapiedra, J. L., Prado, J. L., Fernández, M. H. & Alberdi, M. T. Decoupled ecomorphological evolution and diversification in Neogene-Quaternary horses. *Science* **355**, 627-630 (2017).

4 Pires, M. M., Silvestro, D. & Quental, T. B. Continental faunal exchange and the asymmetrical radiation of carnivores. *Proceedings of the Royal Society B: Biological Sciences* **282**, 20151952 (2015).

5 Pires, M. M., Silvestro, D. & Quental, T. B. Interactions within and between clades shaped the diversification of terrestrial carnivores. *Evolution* **71**, 1855-1864 (2017).

6 Fraser, D. & Lyons, S. K. Biotic interchange has structured Western Hemisphere mammal communities. *Global Ecol. Biogeogr.* **26**, 1408-1422, doi:10.1111/geb.12667 (2017).

7 Fraser, D. & Lyons, S. K. Mammal community structure through the Paleocene-Eocene Thermal Maximum. *Am. Nat.* **196**, 1-20 (2020).

8 Faurby, S. & Svenning, J.-C. The asymmetry in the Great American Biotic Interchange in mammals is consistent with differential susceptibility to mammalian predation. *Global Ecol. Biogeogr.* **25**, 1443-1453, doi:10.1111/geb.12504 (2016).

9 Kempf, H. L., Castro, I. O., Dineen, A. A., Tyler, C. L. & Roopnarine, P. D. Comparisons of Late Ordovician ecosystem dynamics before and after the Richmondian invasion reveal consequences of invasive species in benthic marine paleocommunities. *Paleobiology* **46**, 320-336 (2020).

10 McCreless, E. E. *et al.* Past and estimated future impact of invasive alien mammals on insular threatened vertebrate populations. *Nat Commun* **7** (2016).

11 Sax, D. F. & Gaines, S. D. Species invasions and extinction: the future of native biodiversity on islands. *Proceedings of the National Academy of Sciences* **105**, 11490-11497 (2008).

12 Fraser, D. *et al.* Investigating Biotic Interactions in Deep Time. *Trends Ecol. Evol.* **36**, 61-75 (2020).

13 Tabuce, R., Clavel, J. & Antunes, M. T. A structural intermediate between triisodontids and mesonychians (Mammalia, Acreodi) from the earliest Eocene of Portugal. *Naturwissenschaften* **98**, 145-155 (2011).

14 Rose, K. D. *The beginning of the age of mammals*. (JHU Press, 2006).

15 Missiaen, P. An updated mammalian biochronology and biogeography for the early Paleogene of Asia. *Vertebrata Palasiatica* **49**, 29 (2011).

16 Lofgren, D. L., Lillegraven, J.A., Clemens, W.A., Gingerich, P.D. & Williamson, T.A. in *Late Cretaceous and Cenozoic mammals of North America: biostratigraphy and biochronology* (ed M.O. Woodburne) 43–105 (Columbia University Press, 2004).

17 McKenna, M. C. & Bell, S. K. *Classification of Mammals Above the Species Level*. (Columbia University Press, 1997).

18 Lucas, S. G. in *Evolution of Tertiary mammals of North America* (eds C. M. Janis, K. M. Scott, & L. L. Jacobs and) 274-283 (1998).

19 Lüthje, C. J., Milàn, J. & Hurum, J. r. H. Paleocene tracks of the mammal pantodont genus Titanoides in coal-bearing strata, Svalbard, Arctic Norway. *J. Vert. Paleontol.* **30**, 521-527 (2010).

20 Gingerich, P. D. in *Causes and consequences of globally warm climates in the Early Paleogene* (eds SL Wing, PD Gingerich, B Schmitz, & E Thomas) 463-478 (Geological Society of America, 2003).

21 Bowen, G. J., Koch, P. L., Meng, J., Ye, J. & Ting, S. Age and correlation of fossiliferous late Paleocene–early Eocene strata of the Erlian Basin, Inner Mongolia, China. *American Museum Novitates* **2005**, 1-26 (2005).

22 Smith, T., Rose, K. D. & Gingerich, P. D. Rapid Asia–Europe–North America geographic dispersal of earliest Eocene primate Teilhardina during the Paleocene–Eocene thermal maximum. *Proceedings of the National Academy of Sciences* **103**, 11223-11227 (2006).

23 Simpson, G. G. Holarctic mammal faunas and continental relationships during the Cenozoic. *Geological Society of America Bulletin* **58**, 613-688, doi:10.1130/0016-7606(1947)58[613:hmfacr]2.0.co;2 (1947).

24 Brikiatis, L. The De Geer, Thulean and Beringia routes: key concepts for understanding early Cenozoic biogeography. *J. Biogeogr.* **41**, 1036-1054 (2014).

25 McKenna, M. C. Holarctic landmass rearrangement, cosmic events, and Cenozoic terrestrial organisms. *Annals of the Missouri Botanical Garden* **70**, 459-489 (1983).

26 McKenna, M. C. in *Structure and Development of the Greenland-Scotland Ridge: New Methods and Concepts* Vol. 8 (ed M.H.P. Bott, Saxov, S., Talwani, M., Thiede, J.) 351-399 (Springer, 1983).

27 Tiffney, B. H. The Eocene North Atlantic land bridge: its importance in Tertiary and modern phytogeography of the Northern Hemisphere. *Journal of the Arnold Arboretum* **66**, 243-273 (1985).

28 Jiang, D., Klaus, S., Zhang, Y.-P., Hillis, D. M. & Li, J.-T. Asymmetric biotic interchange across the Bering land bridge between Eurasia and North America. *National Science Review* **6**, 739-745 (2019).

29 Manchester, S. R. Biogeographical relationships of North American tertiary floras. *Annals of the Missouri Botanical Garden* **86**, 472-522 (1999).

30 Manchester, S. R. & Shuang-Xing, G. Palaeocarpinus (extinct Betulaceae) from northwestern China: new evidence for Paleocene floristic continuity between Asia, North America, and Europe. *Int. J. Plant Sci.* **157**, 240-246 (1996).

31 Marincovich, L., Brouwers, E. M., Hopkins, D. M. & McKenna, M. C. in *The Arctic Ocean Region* (ed A. Grantz, Johnson, L., and Sweeney, J.) 403–426 (Geological Society of America, 1990).

32 Gladenkov, A. Y. Onset of connections between the Pacific and Arctic Oceans through the Bering Strait in the Neogene. *Stratigraphy and Geological Correlation* **12**, 175-187 (2004).

33 Rybczynski, N. *et al.* Mid-Pliocene warm-period deposits in the High Arctic yield insight into camel evolution. *Nature Communications* **4**, 1-9 (2013).

620 34 Hutchison, J. H. & Harington, C. A peculiar new fossil shrew (Lipotyphla, Soricidae)
621 from the High Arctic of Canada. *Canadian Journal of Earth Sciences* **39**, 439-443
622 (2002).
623 35 Wang, X., Rybczynski, N., Harington, C. R., White, S. C. & Tedford, R. H. J. S. r. A
624 basal ursine bear (Protarctos abstrusus) from the Pliocene High Arctic reveals Eurasian
625 affinities and a diet rich in fermentable sugars. **7**, 17722 (2017).
626 36 Hulbert, J., Richard C & Harington, C. R. An early Pliocene hipparionine horse from the
627 Canadian Arctic. *Palaeontology* **42**, 1017-1025 (1999).
628 37 Kender, S. *et al.* Closure of the Bering Strait caused mid-Pleistocene transition cooling.
629 *Nature Communications* **9**, 5386 (2018).
630 38 Knudson, K. P. & Ravelo, A. C. North Pacific Intermediate Water circulation enhanced
631 by the closure of the Bering Strait. *Paleoceanography* **30**, 1287-1304 (2015).
632 39 Koblmüller, S. *et al.* Whole mitochondrial genomes illuminate ancient intercontinental
633 dispersals of grey wolves (Canis lupus). *J. Biogeogr.* **43**, 1728-1738 (2016).
634 40 Salis, A. T. *et al.* Lions and brown bears colonized North America in multiple
635 synchronous waves of dispersal across the Bering Land Bridge. *Mol. Ecol.* **31**, 6407-6421
636 (2022).
637 41 McKenna, M. C. Fossil mammals and early Eocene North Atlantic land continuity.
638 *Annals of the Missouri Botanical Garden* **62**, 335-353 (1975).
639 42 Savage, D. E. The Sparnacian-Wasatchian mammalian fauna, Early Eocene, of Europe
640 and North America. *Abh. Hess. Landesamt. Bodenf* **60**, 154-158 (1971).

43 Dawson, M. R. Early Eocene rodents (Mammalia) from the Eureka Sound Group of Ellesmere Island, Canada. *Canadian Journal of Earth Sciences* **38**, 1107-1116, doi:10.1139/cjes-38-7-1107 (2001).

44 Dawson, M. R., McKenna, M. C., Beard, K. C. & Hutchison, J. H. An early Eocene plagiomenid mammal from Ellesmere and Axel Heiberg Islands, Arctic Canada. *Kaupia* **3**, 179-192 (1993).

45 Dawson, M. R., West, R. M., Ramaekers, P. & Hutchison, J. H. New evidence on the palaeobiology of the Eureka Sound Formation, Arctic Canada. *Arctic* **28**, 110-116 (1975).

46 Szalay, F. S. & McKenna, M. C. Beginning of the age of mammals in Asia: the late Paleocene Gashato fauna, Mongolia. Bulletin of the AMNH; v. 144, article 4. *Bulletin of the American Museum of Natural History* **144**, 269-318 (1971).

47 Tucholke, B. E. & McCoy, F. W. in *The Western North Atlantic Region* (eds Peter R. Vogt & Brian E. Tucholke) 589-602 (Geological Society of America, 1986).

48 Blythe, A. E. & Kleinspehn, K. L. Tectonically versus climatically driven Cenozoic exhumation of the Eurasian plate margin, Svalbard: Fission track analyses. *Tectonics* **17**, 621-639 (1998).

49 Müller, R. D. & Spielhagen, R. F. Evolution of the Central Tertiary Basin of Spitsbergen: towards a synthesis of sediment and plate tectonic history. *Palaeogeogr., Palaeoclimatol., Palaeoecol.* **80**, 153-172 (1990).

50 Lee, C., Lehnert, O. & Nowlan, G. Sedimentology, stratigraphy, and clast biostratigraphy of Cretaceous and Tertiary strata, northeastern Ellesmere Island, Nunavut. *Geological Survey of Canada Bulletin* **592**, 115-167 (2008).

663 51 Strauch, F. Die Thule-Landbrücke als Wanderweg und Faunenscheide zwischen Atlantik
664 und Skandik im Tertiär. *Geologische Rundschau* **60**, 381-417 (1970).
665 52 Axelrod, D. I. Biogeography of oaks in the Arcto-Tertiary province. *Annals of the*
666 *Missouri Botanical Garden* **70**, 629-657 (1983).
667 53 Saunders, A. D., Fitton, J.G., Kerr, A.C., Norry, M.J. & Kent, R.W. in *Large igneous*
668 *provinces: continental, oceanic, and planetary flood volcanism* (ed M.F. Coffin J.J.
669 Mahoney) 45-93 (American Geophysical Union, 1997).
670 54 Hohbein, M. W., Sexton, P. F. & Cartwright, J. A. Onset of North Atlantic Deep Water
671 production coincident with inception of the Cenozoic global cooling trend. *Geology* **40**,
672 255-258 (2012).
673 55 Smallwood, J. R. & Gill, C. E. The rise and fall of the Faroe–Shetland Basin: evidence
674 from seismic mapping of the Balder Formation. *Journal of the Geological Society* **159**,
675 627-630 (2002).
676 56 Shaw Champion, M., White, N., Jones, S. & Lovell, J. Quantifying transient mantle
677 convective uplift: An example from the Faroe Shetland basin. *Tectonics* **27** (2008).
678 57 Hartley, R. A., Roberts, G. G., White, N. & Richardson, C. Transient convective uplift of
679 an ancient buried landscape. *Nature Geoscience* **4**, 562-565 (2011).
680 58 Beard, K. C. & Dawson, M. R. Intercontinental dispersal of Holarctic land mammals near
681 the Paleocene/Eocene boundary; paleogeographic, paleoclimatic and biostratigraphic
682 implications. *Bull. Soc. Geol. Fr.* **170**, 697-706 (1999).
683 59 Dinerstein, E. *The return of the unicorns: the natural history and conservation of the*
684 *greater one-horned rhinoceros.* (Columbia University Press, 2003).

60 Havmøller, R. G. *et al.* Will current conservation responses save the critically endangered Sumatran rhinoceros Dicerorhinus sumatrensis? *Oryx* **50**, 355-359 (2016).

61 Khan, M. K. B. M. & Strien, N. J. v. *Asian rhinos: status survey and conservation action plan*. Vol. 32 (IUCN, 1997).

62 Rookmaaker, K. & Antoine, P.-O. New maps representing the historical and recent distribution of the African species of rhinoceros: Diceros bicornis, Ceratotherium simum and Ceratotherium cottoni. *Pachyderm* **52**, 91-96 (2012).

63 Prothero, D. R. *The evolution of North American rhinoceroses*. (Cambridge University Press, 2005).

64 Antoine, P.-O. *et al.* A new rhinoceros clade from the Pleistocene of Asia sheds light on mammal dispersals to the Philippines. *Zool. J. Linn. Soc.* **194**, 416-430 (2022).

65 Robertson, P. & Mason, G. D. Shatter cones from Haughton Dome, Devon Island, Canada. *Nature* **255**, 393-394 (1975).

66 Jessberger, E. K. Ar-40-Ar-39 dating of the Haughton impact structure. *Meteoritics* **23**, 233-234 (1988).

67 Omar, G. *et al.* Fission-track dating of Haughton astrobleme and included biota, Devon Island, Canada. *Science* **237**, 1603-1605 (1987).

68 Sherlock, S. C. *et al.* Re□evaluating the age of the Haughton impact event. *Meteoritics & Planetary Science* **40**, 1777-1787 (2005).

69 Young, K. E. *et al.* Impact thermochronology and the age of Haughton impact structure, Canada. *Geophys. Res. Lett.* **40**, 3836-3840 (2013).

70 Erickson, T. M. *et al.* Resolving the age of the Haughton impact structure using coupled 40Ar/39Ar and U-Pb geochronology. *Geochim. Cosmochim. Acta* **304**, 68-82 (2021).

71 Hickey, L. J., Johnson, K. R. & Dawson, M. R. The stratigraphy, sedimentology, and fossils of the Haughton Formation: a post□impact crater□fill, Devon Island, NWT, Canada. *Meteoritics* **23**, 221-231 (1988).

72 Dawson, M. R. Oreolagus and other Lagomorpha (Mammalia) from the Miocene of Colorado, Wyoming, and Oregon. *University Colorado Studies Earth Sciences* **1**, 1-36 (1965).

73 Martin, J. E. A new and unusual shrew (Soricidae) from the Miocene of Colorado and South Dakota. *J. Paleontol.* **3**, 636-641 (1978).

74 Rybczynski, N., Dawson, M. R. & Tedford, R. H. J. N. A semi-aquatic Arctic mammalian carnivore from the Miocene epoch and origin of Pinnipedia. **458**, 1021 (2009).

75 Rabi, M., Bastl, K., Botfalvai, G., Evanics, Z. & Peigné, S. A new carnivoran fauna from the late Oligocene of Hungary. *Palaeobiodiversity and Palaeoenvironments* **98**, 509-521 (2018).

76 Whitlock, C. & Dawson, M. R. Pollen and Vertebrates of the Early Neogene Haughton Formation, Devon Island, Arctic Canada. *Arctic* **43**, 324-330 (1990).

77 Frisch, T. & Thorsteinsson, R. Haughton astrobleme: A mid-Cenozoic impact crater Devon Island, Canadian arctic archipelago. *Arctic*, 108-124 (1978).

78 Stadler, T. Sampling-through-time in birth–death trees. *J. Theor. Biol.* **267**, 396-404 (2010).

79 Wright, A. M., Bapst, D. W., Barido-Sottani, J. & Warnock, R. C. Integrating fossil observations into phylogenetics using the fossilized birth–death model. *Annual Review of Ecology, Evolution, and Systematics* **53**, 251-273 (2022).

80 Höhna, S., Landis, M. J. & Heath, T. A. Phylogenetic inference using RevBayes. *Current protocols in bioinformatics* **57**, 6.16. 11-16.16. 34 (2017).

81 Matzke, N. J. Probabilistic historical biogeography: new models for founder-event speciation, imperfect detection, and fossils allow improved accuracy and model-testing. *Frontiers in Biogeography* **5**, 242-248 (2013).

82 Matzke, N. J. Model Selection in Historical Biogeography Reveals that Founder-event Speciation is a Crucial Process in Island Clades. *Syst. Biol.* **63**, 951-970 (2014).

83 Stochastic mapping under biogeographical models (2016).

84 Ree, R. H. & Smith, S. A. Maximum Likelihood Inference of Geographic Range Evolution by Dispersal, Local Extinction, and Cladogenesis. *Syst. Biol.* **57**, 4-14, doi:10.1080/10635150701883881 (2008).

85 Owen, R. *On the archetype and homologies of the vertebrate skeleton*. (author, 1848).

86 Owen, R. Odontography. London. *UK: Hippolyte Bailliere* (1845).

87 Gray, J. E. On the natural arrangement of vertebrate mammals. *London medical repository* **15**, 296-310 (1821).

88 Abel, O. *Kritische Untersuchungen über die paläogenen Rhinocerotiden Europas*. (Hölder, 1910).

89 Uhlig, U. Die Rhinocerotoidea (Mammalia) aus der unteroligozänen Spaltenfüllung Möhren 13 bei Treuchtlingen in Bayern. Abhandlungen der Bayerischen Akademie der Wissenschafen, Mathematisch-Naturwissenschaftliche Klasse, Neue Folge. *Munich* **170**, 1254 (1999).

90 Böhme, M. *et al.* Na Duong (northern Vietnam)-an exceptional window into Eocene ecosystems from Southeast Asia. *Zitteliana. Reihe A, Mitteilungen der Bayerischen Staatssammlung fu□r Pala□ontologie und Geologie* **53**, 121-167 (2013).

91 Antoine, P.-O. *et al.* A revision of Aceratherium blanfordi Lydekker, 1884 (Mammalia: Rhinocerotidae) from the Early Miocene of Pakistan: postcranials as a key. *Zool. J. Linn. Soc.* **160**, 139-194 (2010).

92 Becker, D., Antoine, P.-O. & Maridet, O. A new genus of Rhinocerotidae (Mammalia, Perissodactyla) from the Oligocene of Europe. *Journal of Systematic Palaeontology* **11**, 947-972 (2013).

93 Tissier, J., Antoine, P.-O. & Becker, D. New material of Epiaceratherium and a new species of Mesaceratherium clear up the phylogeny of early Rhinocerotidae (Perissodactyla). *Royal Society Open Science* **7**, 200633 (2020).

94 Antoine, P.-O., Alférez, F. & Iñigo, C. A new elasmotheriine (Mammalia, Rhinocerotidae) from the Early Miocene of Spain. *Comptes Rendus Palevol* **1**, 19-26 (2002).

95 Kosintsev, P. *et al.* Evolution and extinction of the giant rhinoceros Elasmotherium sibiricum sheds light on late Quaternary megafaunal extinctions. *Nature ecology & evolution* **3**, 31-38 (2019).

96 Eberle, J. *et al.* The First Tertiary fossils of mammals, turtles, and fish from Canada's Yukon. *American Museum Novitates* **2019**, 1-28 (2019).

97 Grímsson, F. & Denk, T. Fagus from the Miocene of Iceland: systematics and biogeographical considerations. *Rev. Palaeobot. Palynol.* **134**, 27-54 (2005).

98 Denk, T., Grímsson, F. & Zetter, R. Episodic migration of oaks to Iceland: Evidence for a North Atlantic "land bridge" in the latest Miocene. *Am. J. Bot.* **97**, 276-287 (2010).

99 Stepien, C. A. & Haponski, A. E. in *Biology and Culture of Percid Fishes: Principles and Practices* (ed Konrad Dabrowski Patrick Kestemont, Robert C. Summerfelt) 3-60 (Springer, 2015).

100 Haponski, A. E. & Stepien, C. A. Phylogenetic and biogeographical relationships of the Sander pikeperches (Percidae: Perciformes): patterns across North America and Eurasia. *Biol. J. Linn. Soc.* **110**, 156-179 (2013).

101 Stepien, C., Behrmann-Godel, J, Bernatchez, L. in *Biology of perch* (ed Moyer G Couture P) Ch. 2, 7–46 (CRC Press, 2015).

102 Vornam, B., Decarli, N. & Gailing, O. Spatial distribution of genetic variation in a natural beech stand (Fagus sylvatica L.) based on microsatellite markers. *Conserv. Genet.* **5**, 561-570 (2004).

103 Straume, E. O., Gaina, C., Medvedev, S. & Nisancioglu, K. H. Global Cenozoic paleobathymetry with a focus on the Northern Hemisphere oceanic gateways. *Gondwana Research* **86**, 126-143 (2020).

104 Lasabuda, A. P. *et al.* Paleobathymetric reconstructions of the SW Barents Seaway and their implications for Atlantic–Arctic ocean circulation. *Communications Earth & Environment* **4**, 231 (2023).

105 Jakobsson, M. *et al.* The early Miocene onset of a ventilated circulation regime in the Arctic Ocean. *Nature* **447**, 986-990 (2007).

106 Jokat, W., Lehmann, P., Damaske, D. & Nelson, J. B. Magnetic signature of North-East Greenland, the Morris Jesup Rise, the Yermak Plateau, the central Fram Strait:

797 constraints for the rift/drift history between Greenland and Svalbard since the Eocene.
798 *Tectonophysics* **691**, 98-109 (2016).
799 107 Ehlers, B.-M. & Jokat, W. Paleo-bathymetry of the northern North Atlantic and
800 consequences for the opening of the Fram Strait. *Marine Geophysical Research* **34**, 25-43
801 (2013).
802 108 Engen, Ø., Faleide, J. I. & Dyreng, T. K. Opening of the Fram Strait gateway: A review
803 of plate tectonic constraints. *Tectonophysics* **450**, 51-69 (2008).
804 109 Kristoffersen, Y. in *Geological History of the Polar Oceans: Arctic Versus Antarctic* 63–
805 76 (Springer, 1990).
806 110 Knies, J. & Gaina, C. Middle Miocene ice sheet expansion in the Arctic: Views from the
807 Barents Sea. *Geochemistry, Geophysics, Geosystems* **9** (2008).
808 111 Myhre, A., Thiede, J., Firth, J., Ahagon, N., Black, K., Bloemendal, J., Brass, G.,
809 Bristow, J., Chow, N., Cremer,M. Site 909. *Proceedings of the Ocean Drilling Program.*
810 *Initial Reports. Ocean Drilling Program.* **151**, 159–220 (1995).
811 112 Wold, C. Palaeobathymetric reconstruction on a gridded database: The northern North
812 Atlantic and southern Greenland-Iceland-Norwegian Sea. *Geological Society, London,*
813 *Special Publications* **90**, 271-302 (1995).
814 113 Poore, H., Samworth, R., White, N., Jones, S. & McCave, I. Neogene overflow of
815 northern component water at the Greenland□Scotland Ridge. *Geochemistry, Geophysics,*
816 *Geosystems* **7** (2006).
817 114 Ramsay, A. T., Smart, C. W. & Zachos, J. C. A model of early to middle Miocene deep
818 ocean circulation for the Atlantic and Indian Oceans. *Geological Society, London, Special*
819 *Publications* **131**, 55-70 (1998).

115 Denk, T. *et al.* in *Late Cainozoic floras of Iceland: 15 million years of vegetation and climate history in the northern North Atlantic Topics in Geobiology* (ed Friðgeir Grimsson Thomas Denk , Reinhard Zetter , Leifur A. Símonarson) 647-668 (Springer, 2011).

116 Poore, R. H. *Neogene Epeirogeny and the Iceland Plume* PhD thesis, University of Cambridge, (2008).

117 Eldholm, O., Myhre, A. M., Thiede, J. in *Cenozoic plants and climates of the Arctic* Vol. 127 *NATO ASI Series* (ed H. C. Fisher M. C. Boulter) 35-55 (Springer, Berlin/Heidelberg, 1994).

118 Thiede, J., Eldholm, O. in *Structure and development of the Greenland-Scotland Ridge: New methods and concepts* (ed S. Saxow M. H. P. Bott, M. Talwani, J.Thiede) 445-456 (Plenum, 1983).

119 Trettin, H. in *Geology of the Innuitian Orogen and Arctic Platform of Canada and Greenland* Vol. 3 *Geology of Canada Series* (ed HP Trettin) 59-66 (Geological Survey of Canada, 1991).

120 Oakey, G. N. & Chalmers, J. A. A new model for the Paleogene motion of Greenland relative to North America: Plate reconstructions of the Davis Strait and Nares Strait regions between Canada and Greenland. *Journal of Geophysical Research: Solid Earth* **117** (2012).

121 Zachos, J., Pagani, M., Sloan, L., Thomas, E. & Billups, K. Trends, rhythms, and aberrations in global climate 65 Ma to present. *Science* **292**, 686-693 (2001).

122 Zachos, J. C., Dickens, G. R. & Zeebe, R. E. An early Cenozoic perspective on greenhouse warming and carbon-cycle dynamics. *Nature* **451**, 279-283 (2008).

123 Stein, R. The late Mesozoic□Cenozoic Arctic Ocean climate and sea ice history: A challenge for past and future scientific ocean drilling. *Paleoceanography and Paleoclimatology* **34**, 1851-1894 (2019).

124 Polyak, L. *et al*. History of sea ice in the Arctic. *Quaternary Science Reviews* **29**, 1757–1778 (2010).

125 Brice, K. L., Arthur, M. A. & Marincovich Jr, L. Late Paleocene Arctic Ocean shallow□marine temperatures from mollusc stable isotopes. *Paleoceanography* **11**, 241-249 (1996).

126 O'Brien, C. L. *et al*. The enigma of Oligocene climate and global surface temperature evolution. *Proceedings of the National Academy of Sciences* **117**, 25302-25309 (2020).

127 Thiede, J. *et al.* Late Cenozoic history of the Polar North Atlantic: results from ocean drilling. *Quaternary Science Reviews* **17**, 185-208 (1998).

128 Backman, J. *et al*. Age model and core□seismic integration for the Cenozoic Arctic Coring Expedition sediments from the Lomonosov Ridge. *Paleoceanography* **23** (2008).

129 Moran, K. *et al*. The Cenozoic palaeoenvironment of the Arctic Ocean. *Nature* **441**, 601-605 (2006).

130 Darby, D. A. Ephemeral formation of perennial sea ice in the Arctic Ocean during the middle Eocene. *Nature Geoscience* **7**, 210-213 (2014).

131 St. John, K. Cenozoic ice□rafting history of the central Arctic Ocean: Terrigenous sands on the Lomonosov Ridge. *Paleoceanography* **23** (2008).

132 Stickley, C. E. *et al*. Evidence for middle Eocene Arctic sea ice from diatoms and ice-rafted debris. *Nature* **460**, 376-379 (2009).

133 Eldrett, J. S., Harding, I. C., Wilson, P. A., Butler, E. & Roberts, A. P. Continental ice in Greenland during the Eocene and Oligocene. *Nature* **446**, 176-179 (2007).

134 Tripati, A. K. *et al.* Evidence for glaciation in the Northern Hemisphere back to 44 Ma from ice-rafted debris in the Greenland Sea. *Earth and Planetary Science Letters* **265**, 112-122 (2008).

135 Tripati, A. & Darby, D. Evidence for ephemeral middle Eocene to early Oligocene Greenland glacial ice and pan-Arctic sea ice, Nat. Commun., 9, 1038. *Nature Communications* **9**, 1038 (2018).

136 Westerhold, T. *et al.* An astronomically dated record of Earth's climate and its predictability over the last 66 million years. *Science* **369**, 1383-1387 (2020).

137 Pound, M. J., Haywood, A. M., Salzmann, U. & Riding, J. B. Global vegetation dynamics and latitudinal temperature gradients during the Mid to Late Miocene (15.97–5.33 Ma). *Earth-Sci. Rev.* **112**, 1-22 (2012).

138 Klein, D. R. Comparative ecological and behavioral adaptations of Ovibos moschatus and Rangifer tarandus. *Rangifer* **12**, 47-55 (1992).

139 Hansen, B. & Aanes, R. Kelp and seaweed feeding by High-Arctic wild reindeer under extreme winter conditions. *Polar Res.* **31**, 17258 (2012).

140 Hassan, M. Y. & Haller, J. *Tertiary faunas from Kap Brewster, East Greenland: de Danske ekspeditioner til Østgrønland 1947-52*. (Reitzel, 1953).

141 Wappler, T. *et al.* Before the 'Big Chill': A preliminary overview of arthropods from the middle Miocene of Iceland (Insecta, Crustacea). *Palaeogeogr., Palaeoclimatol., Palaeoecol.* **401**, 1-12 (2014).

142 Wang, X., Flynn, L. J. & Fortelius, M. *Fossil mammals of Asia: Neogene biostratigraphy and chronology*. (Columbia University Press, 2013).

143 Behrensmeyer, A. K., Western, D. & Boaz, D. E. D. New perspectives in vertebrate paleoecology from a recent bone assemblage. *Paleobiology* **5**, 12-21, doi:doi:10.1017/S0094837300006254 (1979).

144 Behrensmeyer, A. K., Kidwell, S. M. & Gastaldo, R. A. Taphonomy and paleobiology. *Paleobiology* **26**, 103-147, doi:10.1666/0094-8373(2000)26[103:tap]2.0.co;2 (2000).

145 Höhna, S. *et al.* RevBayes: Bayesian phylogenetic inference using graphical models and an interactive model-specification language. *Syst. Biol.* **65**, 726-736 (2016).

146 Höhna, S. *et al.* Probabilistic graphical model representation in phylogenetics. *Syst. Biol.* **63**, 753-771 (2014).

147 Barido-Sottani, J. *et al. Estimating a time-calibrated phylogeny of fossil and extant taxa using RevBayes*. .5.2:1--5.2:23 (No commercial publisher, 2020).

148 Heath, T. A., Huelsenbeck, J. P. & Stadler, T. The fossilized birth–death process for coherent calibration of divergence-time estimates. *Proceedings of the National Academy of Sciences* **111**, E2957-E2966 (2014).

149 Stadler, T., Gavryushkina, A., Warnock, R. C., Drummond, A. J. & Heath, T. A. The fossilized birth-death model for the analysis of stratigraphic range data under different speciation modes. *J. Theor. Biol.* **447**, 41-55 (2018).

150 Foote, M. On the probability of ancestors in the fossil record. *Paleobiology* **22**, 141-151 (1996).

151 Lewis, P. O. A likelihood approach to estimating phylogeny from discrete morphological character data. *Syst. Biol.* **50**, 913-925 (2001).

152 Jukes, T. H. & Cantor, C. R. Evolution of protein molecules. *Mammalian protein metabolism* **3**, 21-132 (1969).

153 Drummond, A. J., Ho, S. Y. W., Phillips, M. J. & Rambaut, A. Relaxed phylogenetics and dating with confidence. *PLoS Biol.* **4**, e88 (2006).

154 Troshin PV, P. J., Barton GJ. Java bioinformatics analysis web services for multiple sequence alignment–JABAWS:MSA. *Bioinformatics* **27**, 2001-2002, doi:doi:10.1093/bioinformatics/btr304 (2011).

155 Troshin PV, P. J., Sherstnev A, Barton DL, Madeira F, Barton GJ. JABAWS 2.2 Distributed Web Services for Bioinformatics: Protein Disorder, Conservation and RNA Secondary Structure. *Bioinformatics* **34**, 1939-1940, doi:doi:10.1093/bioinformatics/bty045 (2018).

156 Ree, R. H., Moore, B. R., Webb, C. O. & Donoghue, M. J. A likelihood framework for inferring the evolution of geographic range on phylogenetic trees. *Evolution* **59**, 2299-2311, doi:10.1111/j.0014-3820.2005.tb00940.x (2005).

157 Ronquist, F. Dispersal-vicariance analysis: a new approach to the quantification of historical biogeography. *Syst. Biol.* **46**, 195-203 (1997).

158 Landis, M. J., Matzke, N. J., Moore, B. R. & Huelsenbeck, J. P. Bayesian analysis of biogeography when the number of areas is large. *Syst. Biol.* **62**, 789-804 (2013).

159 Dupin, J. *et al.* Bayesian estimation of the global biogeographical history of the Solanaceae. *J. Biogeogr.* **44**, 887-899 (2017).

Acknowledgements

The Canadian Museum of Nature (CMN; primary workplace of D.F., M.G., and N.R.) resides on the traditional, unceded territory of the Anishinābe Algonquin people who have stewarded the land for thousands of years. We acknowledge that the CMN's scientific research occurs across Canada—from coast to coast to coast—on the territories of the Métis and First Nations people and in Inuit Nunangat. This work was supported by a Natural Sciences and Engineering Research Council of Canada Grant to D.F. (NSERC RGPIN-2018-05305). The field work would not have been possible without the support from the Polar Continental Shelf Program, the Nunavut Planning Comission, and the Nunavut Impact Review Board. This research was also supported by a palaeontology permit from the Government of Nunavut, Department of Culture, Language, Elders and Youth, and with the permission of the Qikiqtani Inuit Association, especially Grise Fiord. Guidance on Inuktitut words and advice on pronunciation were provided by Jarloo Kiguktak. Field research was supported by the CMN and the Carnegie Museum of Natural History. Collections support was provided by K. Shepherd, M. Currie, and S. Rufolo. 3D models were created and edited by A. Tirabasso and A. McDonald.

Author Contributions

D.F. described the specimen, took measurements and photos, performed the phylogenetic analysis, performed the biogeographic analyses, and wrote the manuscript. N.R. was field leader in 2007, 2008, 2009, and 2010, described the specimen, took measurements and photos, and wrote the manuscript. M.G. was part of the field team in 2008, 2009, and 2010, described the specimen, took measurements and photos, and wrote the manuscript. M.R.D was field leader in 1986 when the majority of the rhinocerotid specimen was collected, described the specimen, and took measurements.

Competing Interests

The authors declare no competing interests.

TABLES

TABLE 1. Model fit statistics for the various biogeographic models based on a NALB opening date of 21 Ma.

Model	LnL	numparams	D	e	j	AICc	ΔAIC	AICc_wt
DEC+J	**-108.2**	**3**	**0.005**	**1.00E-12**	**0.09**	**222.9**	**0.00**	**0.77**
DIVALIKE+J	-109.8	3	0.006	0.002	0.07	226.1	3.20	0.16
BAYAREALIKE+J	-110.7	3	0.004	0.004	0.09	227.8	4.90	0.07
DIVALIKE	-126.3	2	0.015	0.008	-	256.9	34.00	3.30E-08
DEC	-130.0	2	0.013	0.011	-	264.3	41.40	8.10E-10
BAYAREALIKE	-140.4	2	0.009	0.072	-	285.1	62.20	2.40E-14

962 **FIGURES**

963

964 **FIGURE 1.** 3D scan of the skull elements of *Epiaceratherium itjilik* spec. nov. Scale is 10 cm.

965

966

967

968

969

970

971

972

973

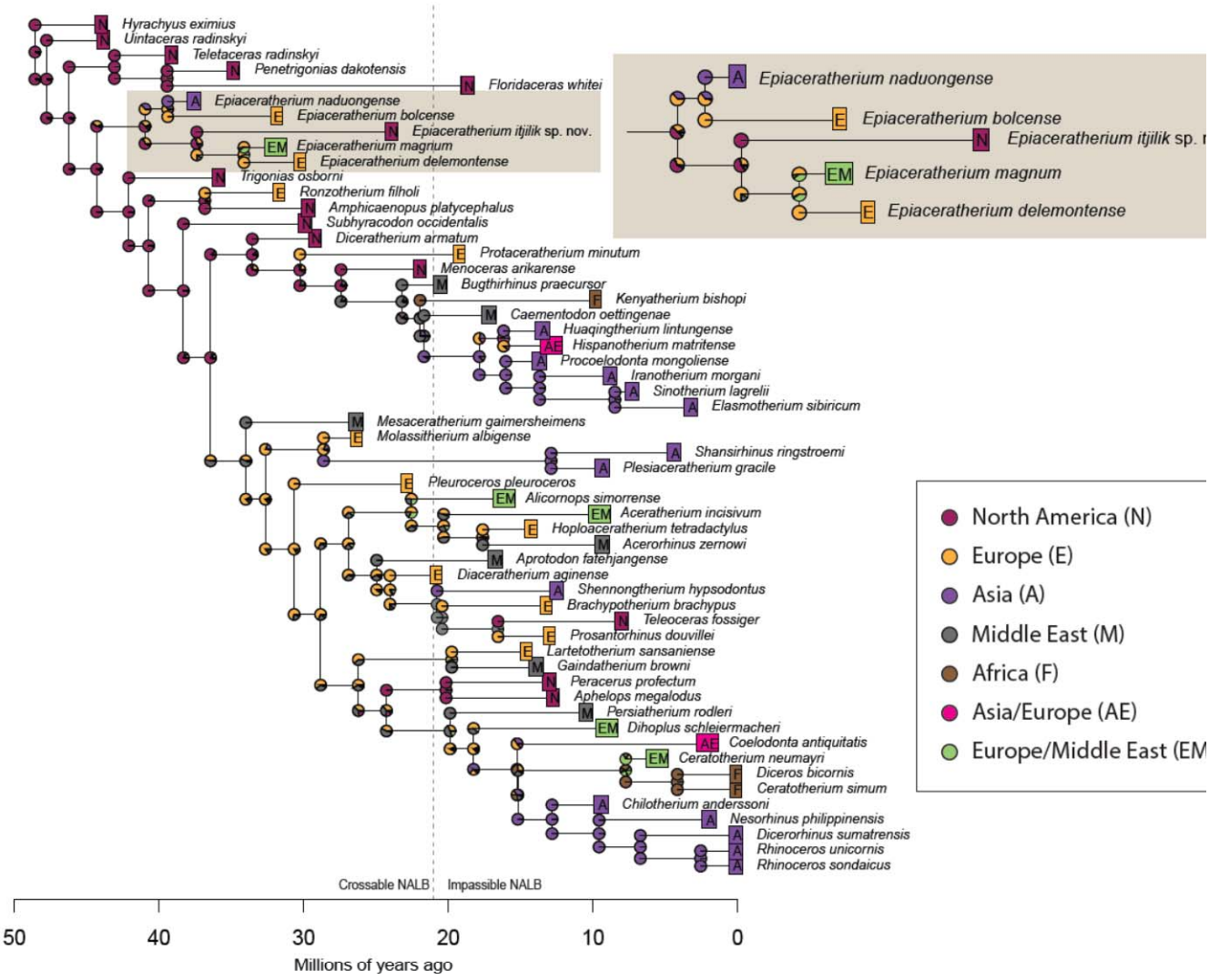

974

975 **FIGURE 2.** Ancestral character estimation of biogeographic regions for rhinocerotids based on a

976 NALB opening date of 21 Ma.

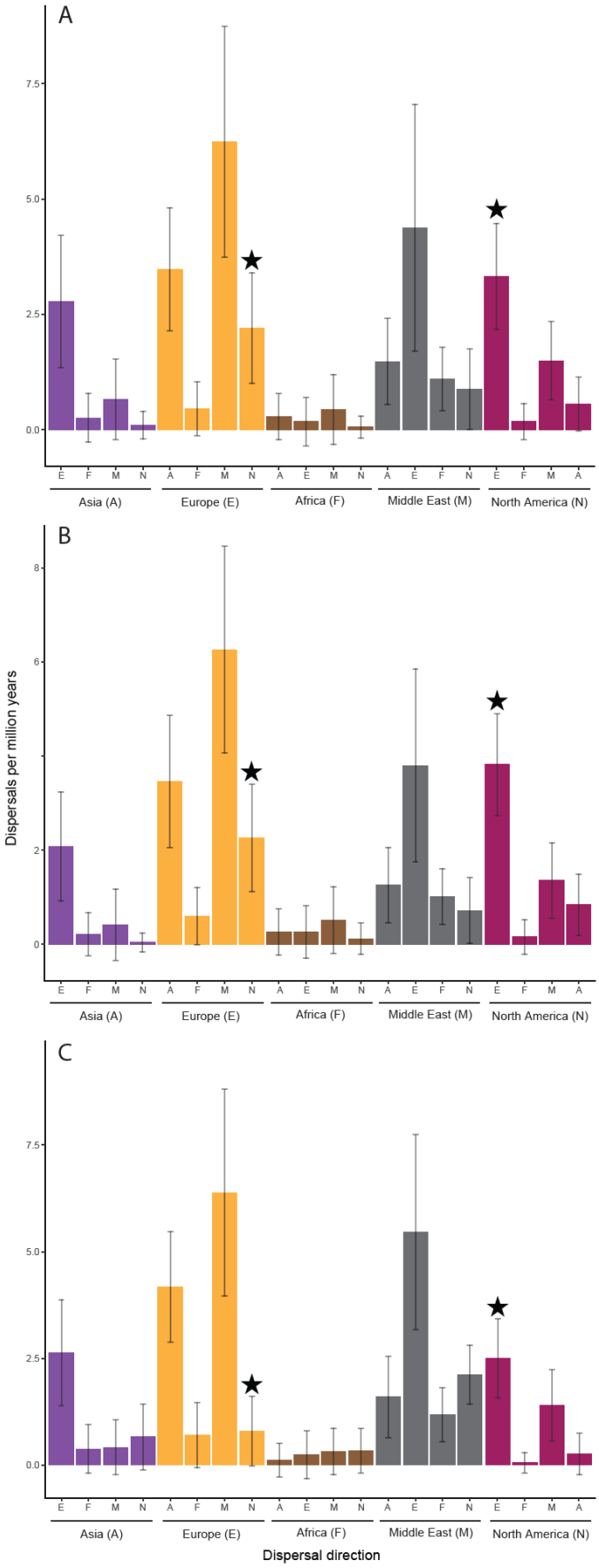

977

978 **FIGURE 3. Dispersals between North America and Europe with relatively high frequency.**
979 Mean counts of dispersal events under (A) an unstratified model, (B) a model limiting dispersal
980 via the North Atlantic after 21 Ma, and (C) a model limiting dispersal via the North Atlantic after
981 35 Ma. Error bars represent standard deviations of counts. Black stars indicate dispersal between
982 North America and Europe, in both directions.

983